

Dark spatial solitons sequence in the biased centrosymmetric photorefractive crystal*

ZHANG Yuhong^{1**} and JIA Xinjuan²

1. College of Opto-Electronic Engineering, Xi'an Technological University, Xi'an 710021, China

2. College of Freshmen, Xi'an Technological University, Xi'an 710021, China

(Received 15 February 2022; Revised 12 June 2022)

©Tianjin University of Technology 2022

We theoretically investigate the evolution of dark screening spatial solitons originating from the quadratic electro-optic effect in biased centrosymmetric photorefractive (CP) crystal by using beam propagation method (BPM). The results indicate that the multiple dark solitons sequence can be obtained in the CP crystal with the odd or even initial conditions. If the initial width of the dark notch is smaller, only a fundamental soliton or a Y-junction soliton pair is generated. When the initial width of the dark notch and the bias electric field are increased, the multiple dark spatial solitons sequence is formed, which realized a progressive transition from a low-order soliton to a higher-order solitons sequence in both odd and even conditions. The solitons characteristic is similar to that of screening solitons in the non-centrosymmetric photorefractive (NCP) crystals.

Document code: A **Article ID:** 1673-1905(2022)10-0601-5

DOI <https://doi.org/10.1007/s11801-022-2024-7>

Photorefractive spatial solitons have become a major field of research in nonlinear optics due to their creation at very low laser power levels and possible applications for optical switching and routing and coupling. They appear in following several different types of media, including non-centrosymmetric photorefractive (NCP) medium, photorefractive polymetric medium, centrosymmetric photorefractive (CP) medium, liquid crystal, and so on. Since SEGEV et al^[1] predicted the existence of spatial solitons in biased potassium lithium tantalate niobate (KLTN) media driven by the quadratic electro-optic effect, the investigations on photorefractive spatial solitons in biased CP crystal have been carried out. In 1998, DELRE et al observed the one-dimensional (1D)^[2] and two-dimensional (2D)^[3] solitons in biased KLTN crystal, and predicted self-focusing and self-trapping of optical beams propagating in unbiased CP crystals in the near-transition paraelectric phase^[4]. In 2006, LI et al^[5] presented the space-charge field with a higher-order nonlinearity and discussed the stability of the fundamental bright and dark soliton in biased CP media while the drift terms were only considered. JI et al investigated spatial gray solitons^[6] in CP crystal and separate spatial solitons pairs in a series of centrosymmetric and non-centrosymmetric hybrid photorefractive crystal circuit^[7] and the effects of temperature on intensity profile and the self-deflection of spatial solitons by numerical simulation in centrosymmetric KLTN crystal^[8-11]. On the other side, ZHAN et al investigated bright and dark solitons^[12], holographic solitons^[13], Manokov solitons^[14], coherently and

incoherently coupled soliton pairs^[15-17], self-deflection^[18] and the effects of temperature^[19] on the intensity profiles of solitons in centrosymmetric paraelectric crystals. The results of researches showed the above spatial solitons can exit in biased CP crystal. The drift component is dominant and the diffusion component affects only the deflection of spatial solitons. In 2017, KATTI et al^[20] theoretically investigated incoherently coupled solitons pair in CP crystals. In 2018, JIANG et al^[21] investigated the propagation and interaction properties of Airy-Gaussian beams in CP media. In addition, lattice solitons were studied in the CP crystal^[22-26]. However, to the best of our knowledge, the dynamical behavior of the dark-notch-bearing beam in bulk CP nonlinear material is unknown yet. Based on Refs.[27—30], the multiple dark solitons can be formed in the NCP crystal. The photoinduced waveguides associated with multiple dark-gray solitons can prove to create reconfigurable optical passive device, such as beam multiplexers and all optical-switching. The number of outputs can be effectively controlled by adjusting the width of the input dark notch and external bias voltage.

Therefore, we employ beam propagation method (BPM) to explore the dynamic behavior of notchbearing beam along the propagation direction in biased CP material with one-photon photorefractive effect. The initial profile of the dark solitons at the entrance of the CP crystal is obtained by solving the nonlinear Schrödinger equation which describes the propagation of the CP spatial solitons. The investigation results illustrate that the splitting of dark spatial solitons is possible in biased CP crystals by

* This work has been supported by the National Foundation of Shaanxi Provincial Department of Education (No.17JK0389).

** E-mail: zhangyh1979@163.com

changing the initial input width of the dark notch. If the full width half maximum (*FWHM*) of the beam intensity is small, only a fundamental soliton or Y-junction solitons pair is generated. When the intensity *FWHM* of the input beam is increased, the solitons beam usually splits into an odd or even number of multiple dark solitons at a proper extra bias voltage.

To study the dynamic behavior of the solitons beam in the CP crystal, we assume that the input beam is uniform along the *y*-axis and is allowed to diffract only along the *x* direction and propagate in a biased CP crystal along the *z*-axis and is linearly polarized along the *x* direction. Meanwhile, another *y*-axis polarized beam that propagates inside the crystals along the *z*-axis serves as the background beam. The CP crystal is assumed to be KLTN with its optical *c*-axis oriented along *x* direction. Moreover, the external bias electric field as well as the polarization of the incident optical beam is also parallel to the *c*-axis.

Theoretically, the solution for a 1D dark spatial soliton propagating along the *z*-axis is described in the CP crystal by the nonlinear Schrödinger equation as

$$\left(\frac{\partial}{\partial z} - \frac{i}{2k} \frac{\partial^2}{\partial x^2}\right) A(x, z) = i \frac{k}{n_e} \Delta n_e A(x, z), \quad (1)$$

where $A(x, z)$ is the slowly varying amplitude of the solitons beam, n_e is unperturbed index of refraction, $k = k_0 n_e = (2\pi/\lambda_0) n_e$, and λ_0 is the vacuum wavelength. The photo-induced change of refractive index^[1-3] in centrosymmetric media is given by

$$\Delta n_e = -0.5 n_e^3 g_{\text{eff}} \varepsilon_0^2 (\varepsilon_r - 1)^2 E_{\text{sc}}^2, \quad (2)$$

where E_{sc} is the space charge field in the material resulting from the external bias electric field and the displacement of charge caused by the optical intensity, g_{eff} is the effective quadratic electro-optic coefficient, and ε_0 and ε_r are the vacuum and relative dielectric constants, respectively.

In the steady state, based on the band-transport model of Kukhtarev, the space charge field^[18] E_{sc} in a biased CP crystal can be expressed as

$$E_{\text{sc}} = E_0 \frac{I_\infty + I_d + I_b}{I + I_d + I_b} - \frac{k_B T}{e} \frac{\partial I / \partial x}{(I + I_b + I_d)}, \quad (3)$$

where $I = |A|^2$ is input solitons intensity, $I_\infty = I(\infty, z)$, I_d is dark irradiation, I_b is background intensity, and E_0 is the external electric field. If the spatial extent of the soliton beam is much less than the *x*-width l of crystal, E_0 is approximately given by V/l , where V is the electric potential applied to the crystal between the electrodes separated by distance l . According to Ref.[18], the diffusion component only affects the self-deflection of spatial solitons. So, under a strong bias field condition and for broad incident beams, the drift component of the current in the medium will be dominant, thus the diffusion effects can be neglected^[17,18].

We employ the following dimensionless coordinates and variables of $A = [2\eta(I_d + I_b)/n_e]^{1/2} U$, $\xi = x/x_0$, $\zeta = z/(kx_0^2)$, where x_0 is an arbitrary spatial width. Thus the normal-

ized slowly varying envelope $U(\xi, \zeta)$ obeys the following dynamical evolution equation

$$\frac{\partial U(\xi, \zeta)}{\partial \zeta} - \frac{i}{2} \frac{\partial^2 U(\xi, \zeta)}{\partial \xi^2} + i\beta \left(\frac{1 + |U_\infty|^2}{1 + |U|^2} \right)^2 u(\xi, \zeta) = 0, \quad (4)$$

where $\beta = \frac{1}{2} k_0^2 n_e^4 x_0^2 g_{\text{eff}} \varepsilon_0^2 (\varepsilon_r - 1)^2 (V/l)^2$.

We seek solitons solution of Eq.(4) in the form of $U(\xi, \zeta) = r^{1/2} u(\xi) \exp(i\Gamma\zeta)$. Substituting this form of $U(\xi, \zeta)$ into Eq.(4) yields

$$u''(\xi) = 2\Gamma u(\xi) + 2\beta \left(\frac{1+r}{1+r|u(\xi)|^2} \right)^2 u(\xi), \quad (5)$$

where r is the ratio of the peak value of the intensity of soliton to the sum of background intensity I_b and dark irradiances I_d , $u(\xi)$ is the soliton amplitude normalized to the square root of $(I_b + I_d)$, and Γ is the nonlinearity-induced shift of the propagation constant.

We numerically integrate Eq.(5) and apply the boundary conditions of dark soliton $u'(\infty) = u''(\infty) = 0$, $u(\infty) = 1$ to obtain

$$\Gamma = -\beta, \quad (6)$$

$$u''(\xi) = -2\beta [u^2(\xi) + \frac{(1+r)^2}{r} \frac{1}{1+r|u|^2} - \frac{2r+1}{r}]. \quad (7)$$

We integrate Eq.(5) numerically for various values of r by using the fourth Runge-Kutta algorithm and combine with initial conditions of $u'^2(0) = -2\beta r$ and $u(0) = 0$ to yield the spatial intensity profile of the fundamental dark solitons. The condition necessary for dark solitons is $\beta < 0$, i.e., $g_{\text{eff}} < 0$. The normalized fundamental dark soliton intensity profile is shown in Fig.1. It illustrates that for the fixed extra bias voltage, the greater r value is, the wider the *FWHM* of the dark solitons is.

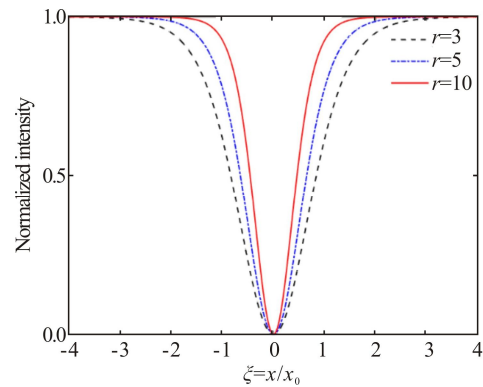


Fig.1 Normalized dark solitons intensity versus ξ for external bias voltage of 800 V

Fig.2 shows the existence curves of the fundamental dark solitons in the biased CP crystal. The existence curves illustrate that intensity *FWHM* of the fundamental dark solitons is the function of the ratio r of solitons peak intensity I_M to the sum of I_d and I_b and external bias voltage V . For the given extra bias voltage, when ration r is smaller than ~ 1 , intensity *FWHM* of the dark solitons sharply reduces. When ration r is greater than ~ 2 , the width of solitons changes slowly and tends to invariable.

In addition, when the r is fixed, the higher the external bias voltage V is, narrower the $FWHM$ of dark solitons is.

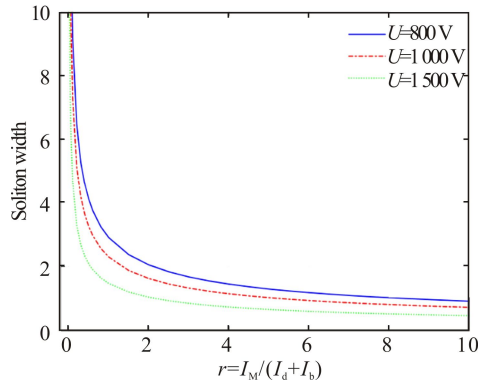


Fig.2 Soliton existence curves with different extra bias voltages

In the following simulations, the crystal-dependent parameters of the biased centrosymmetric crystal are those of the KLTN crystal extracted from the same boule^[6], i.e., $\epsilon_0 = 8.85 \times 10^{-12} \text{ C}^2/\text{N} \cdot \text{m}^2$, $\epsilon_r = 4000$, $n_e = 2.2$, $g_{\text{eff}} = -0.12 \text{ m}^4/\text{C}^2$, $\lambda_0 = 0.5 \mu\text{m}$, $E_0 = V/l = 800 \text{ V/cm}$, $x_0 = 10 \mu\text{m}$, $r = 5$, and $z = 1 \text{ cm}$.

In numerical calculation, while the initial input width of the dark notch is increased, the transform from a lower-order solitons to the higher-order solitons can be realized. Firstly, we numerically calculate $U(\xi, 0)$ by solving Eq.(5) with the fourth Rung-Kutta method to obtain the functional dark solitons and then enlarge the intensity $FWHM$ of the dark solitons. Next, Eq.(4) is solved numerically by BPM to obtain the dynamic evolution process of the multiple solitons inside the biased CP crystal. To ensure the accuracy of BPM, the step size $d\xi$ of each longitudinal section is set as 0.03, i.e., $dz = 1 \mu\text{m}$ and the calculated relative and absolute errors are 10^{-10} in the simulation.

Dark solitons can be obtained by launching an optical beam into a biased CP medium with phase jump and amplitude jump initial conditions. The phase jump initial condition provides a π phase jump in the centre of a beam while keeping the amplitude uniform across the beam. The amplitude jump initial condition is the even initial condition, which provides an amplitude depression at the centre and an even symmetry in the phase of the beam. In this paper, we simulate numerically the dynamic evolution behavior of the dark notch generated by the two initial conditions inside the biased CP crystal in the steady state regime.

(a) Odd initial condition

Under the phase jump initial condition, a fundamental dark solitons solution of Eq.(4) is obtained, while the ratio of soliton peak intensity to dark irradiance is $r = 5$. Under the applied trapping voltage of 800 V, $FWHM$ of the fundamental dark solitons is $12.9 \mu\text{m}$, and the intensity profiles of the fundamental dark solitons at various output planes are shown in Fig.3(a). From Fig.3(a), the intensity $FWHM$ of the fundamental dark solitons doesn't change with the transmission distance.

When we increase input width of the dark notch and the value of extra bias voltage, a pair of gray solitons appears symmetrically on both sides of the central dark solitons. A triple-soliton structure shown in Fig.3(b) is generated with the width of the dark notch of $\Delta x = 50 \mu\text{m}$ and applied trapping voltage of $V = 900 \text{ V}$. The minimum intensities of the two side lobes are not zero. Following this approach, if we increase further intensity $FWHM$ of input beam, we can observe more and more pairs of side lobes developing with less visibility at the higher extra bias voltage. For example, Fig.3(c) shows the five-splitting structure that is found for $\Delta x = 80 \mu\text{m}$ at an applied trapping voltage of $V = 1100 \text{ V}$. If the width of initial input dark notch is further increased, a secondary set of lobes with less visibility symmetrically starts to appear on the two sides of the triple-solitons structure with the higher applied trapping voltage. Thus it can be obviously seen that the broader odd-phased beam tends to split into the odd-number of multiple dark spatial solitons in odd initial condition.

(b) Even initial condition

Under the amplitude jump initial condition, the dark notch always tends to split into even-number sequence dark spatial solitons. When the intensity $FWHM$ of initial dark notch is small, a Y-junction solitons pair is formed. For example, Fig.4(a) shows dynamic behavior of a Y-junction solitons pair for $\Delta x_2 = 40 \mu\text{m}$ at the applied bias voltage of 900 V. The width of each lobe and the depth of the intensity are equal. As the $FWHM$ of the dark notch and the applied extra bias voltage are further increased, in a manner similar to that of an odd-phased beam, more secondary sets of lobes appear symmetrically on two sides of the Y-junction soliton splitting. Fig.4(b) and Fig.4(c) show the four splitting and six splitting for $\Delta x_4 = 60 \mu\text{m}$ at an applied extra voltage of 1000 V and for $\Delta x_6 = 90 \mu\text{m}$ at an applied extra voltage of 1300 V, respectively. If the width of the dark notch and the value of corresponding applied extra bias voltage are increased further, more solitons pairs with less visibility will appear in two sides, forming the higher-order even-number of multiple dark spatial solitons.

In general, from Fig.3 and Fig.4, it is clearly seen that the generation of higher-order solitons mainly depends on the initial width of the dark notch for both odd and even initial conditions. When the initial width of the dark notch is enlarged, more solitons pairs with less visibility are generated in two sides far away from the center.

In summary, a theoretical study on the dynamics of multiple dark solitons formation is presented. The obtained results have indicated that the multiple dark solitons exist in biased CP crystal arising from a single dark notch. The generation of multiple dark spatial solitons is dependent on the initial input width of the dark notch and the external bias field. The number of solitons increases with the width of the initial dark notch. When the width of the dark notch is small, it tends to split into a fundamental dark solitons or Y-junction gray solitons. When the width of the dark notch and the external bias field are

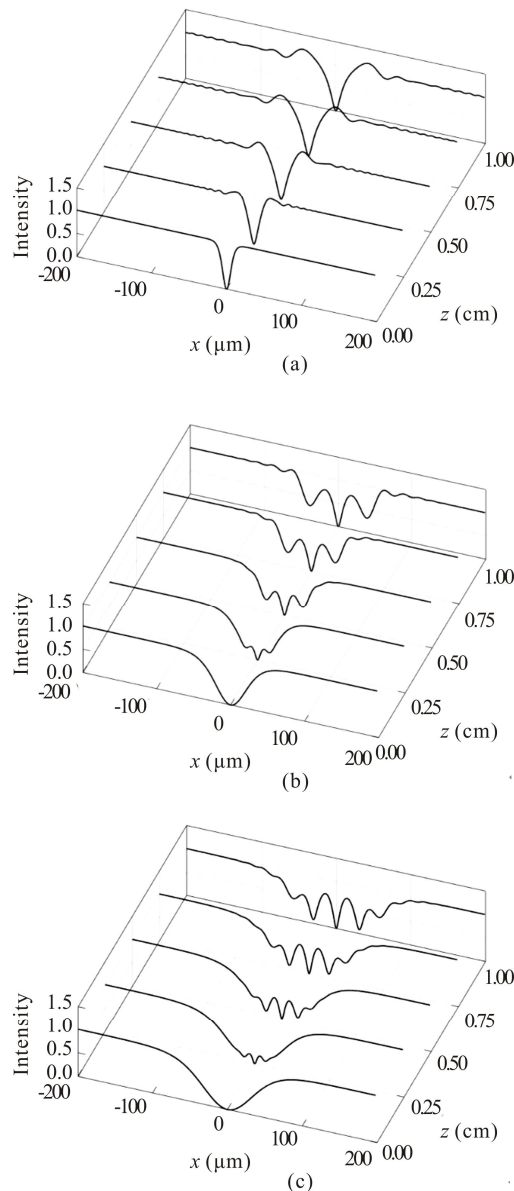


Fig.3 Multiple dark spatial solitons satisfying the odd initial condition: (a) A fundamental dark soliton for $FWHM=12.9 \mu\text{m}$ with $U=800 \text{ V}$; (b) Three-soliton structure for $FWHM=50 \mu\text{m}$ with $U=900 \text{ V}$; (c) Five-soliton structure for $FWHM=80 \mu\text{m}$ with $U=1\,100 \text{ V}$ ($r=5$, $z=1 \text{ cm}$)

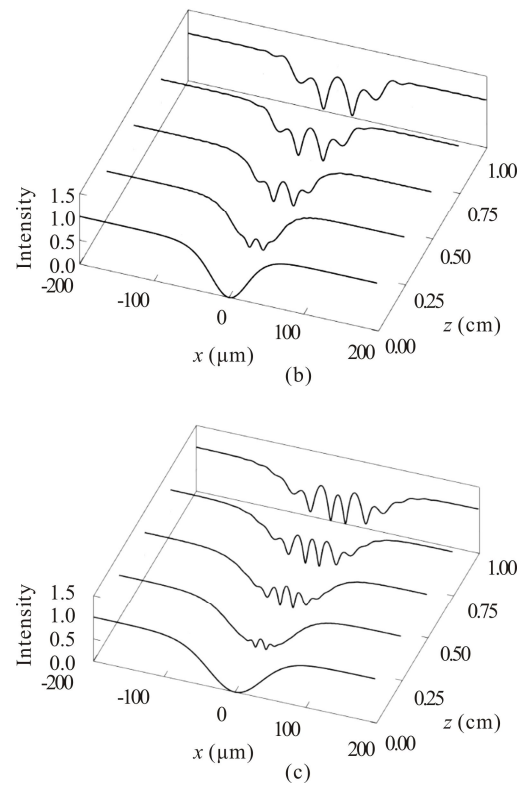
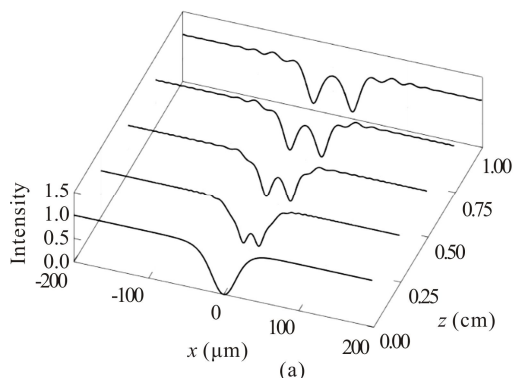


Fig.4 Multiple dark spatial solitons satisfying the even initial condition: (a) A Y-junction solitons pair for $FWHM=40 \mu\text{m}$ with $U=900 \text{ V}$; (b) Three-soliton structure for $FWHM=60 \mu\text{m}$ with $U=900 \text{ V}$; (c) Six-soliton structure for $FWHM=90 \mu\text{m}$ with $U=1\,300 \text{ V}$ ($r=5$, $z=1 \text{ cm}$)

increased, the dark notch tends to split into an odd (or even) number sequence of multiple dark spatial solitons, realizing the transformation from a lower-order solitons to higher-order solitons sequence. When the multiple solitons are generated, the separations between adjacent dark solitons become smaller. The results are similar to multiple dark solitons in the NCP medium^[27-30].

Statements and Declarations

The authors declare that there are no conflicts of interest related to this article.

References

- [1] SEGEV M, AGRAGAT A J. Spatial solitons in centrosymmetric photorefractive media[J]. Optics letters, 1997, 22(17): 1299-1301.
- [2] DELRE E, CROSIGNANI B, TAMBURRINI M, et al. One-dimensional steady-state photorefractive spatial solitons in centrosymmetric paraelectric potassium lithium tantalate niobate[J]. Optics letters, 1998, 23(6): 421-423.
- [3] DELRE E, TAMBURRINI M, SEGEV M, et al. Two-dimensional photorefractive spatial solitons in centrosymmetric paraelectric potassium lithium tantalate nio-

- bate[J]. Applied physics letters, 1998, 73(1): 16-18.
- [4] CROSIGNANI B, DELRE E, PORTO P D, et al. Self-focusing and self-trapping in unbiased centrosymmetric photorefractive media[J]. Optics letters, 1998, 23(12): 912-914.
 - [5] LI J P, LU K Q, ZHAO W, et al. Screening solitons in biased centrosymmetric photorefractive media[J]. Acta photonica sinica, 2006, 35(2): 257-260.
 - [6] JI X M, JIANG Q C, WANG J L, et al. Grey soliton in biased one-photon centrosymmetric photorefractive crystals[J]. Optoelectronics technology, 2011, 31(3): 153-157.
 - [7] JI X M, JIANG Q C, WANG J L, et al. Separate spatial soliton pairs in a series centrosymmetric and non-centrosymmetric hybrid photorefractive crystal circuit[J]. Chinese journal physics, 2012, 50(5): 816-827.
 - [8] SU Y L, JIANG Q C, JI X M. Temperature effects on the self-deflection of bright screening solitons in centrosymmetric photorefractive crystals[J]. Chinese journal physics, 2010, 48(6): 777-782.
 - [9] JI X M, JIANG Q C, WANG J L, et al. Theoretical study of the temporal behavior of one-dimensional bright spatial solitons in biased centrosymmetric photorefractive crystals[J]. Physica scripta, 2011, 83(2): 025404.
 - [10] JIANG Q C, SU Y L, JI X M. Temporal analysis of low-amplitude screening spatial solitons due to two-photon photorefractive effect[J]. Optics & laser technology, 2011, 43(1): 91-94.
 - [11] JI X M, JIANG Q C, SU Y L, et al. Temporal behavior of the screening grey spatial solitons in one-photon centrosymmetric and noncentrosymmetric photorefractive crystals[J]. Infrared and laser engineering, 2013, 42(1): 63-68.
 - [12] ZHAN K Y, HOU C F, TIAN H, et al. Spatial solitons in centrosymmetric photorefractive crystals due to the two-photon photorefractive effect[J]. Journal of optics, 2010, 12(1): 015203.
 - [13] ZHAN K Y, HOU C F, TIAN H, et al. Holographic solitons in centrosymmetric photorefractive crystals[J]. Optics & laser technology, 2010, 42(4): 669-673.
 - [14] ZHAN K Y, HOU C F, TIAN H, et al. Manakov solitons in centrosymmetric photorefractive crystals due to two-photon photorefractive effect[J]. Physics letters A, 2010, 374(10): 1242-1245.
 - [15] ZHAN K Y, HOU C F, TIAN H, et al. Incoherently coupled Gaussian soliton pairs in biased centrosymmetric photorefractive crystals[J]. Optics & laser technology, 2010, 42(7): 1176-1179.
 - [16] ZHAN K Y, HOU C F, ZHANG Y. Incoherently coupled spatial soliton families in centrosymmetric two-photon photorefractive crystals[J]. Journal of optics, 2010, 12(3): 035208.
 - [17] HAO L L, HOU C F, WANG X X, et al. Coherently coupled bright-bright screening soliton pairs in biased centrosymmetric photorefractive crystals[J]. Optik, 2016, 127(15): 5928-5934.
 - [18] ZHAN K Y, HOU C F, DU Y W. Self-deflection of steady-state bright spatial solitons in biased centrosymmetric photorefractive crystals[J]. Optics communications, 2010, 283(1): 138-141.
 - [19] ZHAN K Y, HOU C F, PU S Z. Temporal behavior of spatial solitons in centrosymmetric photorefractive crystals[J]. Optics & laser technology, 2011, 43(7): 1274-1278.
 - [20] KATTI A, YADAV R A, SINGH D P. Theoretical investigation of incoherently coupled solitons in centrosymmetric photorefractive crystals[J]. Optik, 2017, 136: 89-106.
 - [21] JIANG Q H, SU Y L, MA Z W, et al. Propagation properties of Airy-Gaussian beams in centrosymmetric photorefractive media[J]. Journal of modern optics, 2018, 65(19): 2243-2249.
 - [22] ZHAN K Y, HOU C F. Gap solitons supported by optical lattices in biased centrosymmetric photorefractive crystals[J]. Optics communications, 2012, 285(17): 3649-3653.
 - [23] CHEN W J, LU K Q, HUI J L, et al. Localized surface waves at the interface between linear dielectric and biased centrosymmetric photorefractive crystals[J]. Optics express, 2013, 21(13): 15595-15602.
 - [24] HUI J L, LU K Q, CHEN W J, et al. Optical surface waves supported by the interface between a metal and a biased centrosymmetric photorefractive crystal[J]. Optics communications, 2014, 332: 327-331.
 - [25] LU K Q, YU H M, CHEN W J, et al. Defect modes supported by optical lattices in biased centrosymmetric photorefractive crystals[J]. Optical quantum electronics, 2015, 47(8): 2709-2716.
 - [26] FENG J P, QIN Y L, WANG Y Y, et al. Defect solitons supported by two-dimensional lattice potentials in biased centrosymmetric photorefractive crystals with saturable self-focusing nonlinearity[J]. Laser physics, 2020, 30(6): 065401.
 - [27] ZHANG Y H, LU K Q, GUO J B, et al. Steady-state multiple dark photovoltaic spatial solitons[J]. European physics journal D, 2012, 66(3): 65.
 - [28] ZHANG Y H, LU K Q, GUO J B, et al. Formation of multiple dark photovoltaic spatial solitons[J]. Pramana-journal of physics, 2012, 78(2): 265-275.
 - [29] ZHANG Y H, HU X H, LU K Q, et al. Steady-state multiple dark spatial solitons in closed-circuit photovoltaic media[J]. Journal of optical technology, 2013, 80(3): 135-141.
 - [30] ZHANG Y H, SU W, DUAN C L, et al. Steady state multiple dark spatial solitons in the biased photorefractive-photovoltaic crystals[J]. Optoelectronics letters, 2018, 14(5): 0367-0371.